Clays and Clay Minerals, Vol. 52, No. 1, 130–137, 2004.

KAOLIN MINERALS FROM CHINMEN ISLAND (QUEMOY)

PEI YUAN CHEN[1], MING KUANG WANG[2,*], DENG SHIU YANG[2] AND SHYUN SHENG CHANG[3]

[1] Department of Earth Science, National Normal University, Taipei, Taiwan, 106
[2] Department of Agricultural Chemistry, National Taiwan University, Taipei, Taiwan, 106
[3] Central Geological Survey, Ministry of Economic Affairs, Taipei, Taiwan, 235

Abstract—Chinmen Island is located in the west of the Taiwan Strait, 15 km from the coast of mainland China. Mesozoic granitic gneiss forms the basement rocks of the island. High-defect kaolin deposits, both major sedimentary and minor residual types of clays, have been mined for ceramic uses for many years. The objectives of this study were to characterize the kaolin deposits and to discuss the genesis of kaolin minerals on the island. The kaolin samples were characterized by X-ray diffraction and transmission and scanning electron microscopy. In general, the particle-size distribution of the sedimentary kaolin was 0.5–5.0% sand, 15–55% silt and 30–85% clay. In the clay fraction, the ratio of kaolinite to illite ranged from 9:1 to 3:1. The sedimentary kaolin materials were originally transported by river from mainland China. Kaolinite occurred generally as pseudo-hexagonal platelets of ~1 μm in diameter. The residual kaolin minerals resulted from the argillization of granitoid rocks by *in situ* weathering which possibly occurred during the Pleistocene. The residual kaolin contained more tubular halloysite.

Key Words—Chinmen Island, Halloysite, Kaolin Deposits, Kaolinite.

INTRODUCTION

Chinmen Island is located in the west of the Taiwan Strait and is ~15 km from the coast of Fukien Province (Figure 1). It is the largest of the islands near the Hsiamen (Amoy) Harbor. The depth of the Strait between the harbor and the island is generally <10 m in most parts. The climate is subtropical with an average annual temperature of 21°C and precipitation of 1000 mm.

Chinmen Island is shaped like a dumb-bell (Figure 1) and the basement rocks crop out mainly in two low hilly regions on the western and eastern sides of the island. The highest summit is Mount Taiwushan (253 m elevation) in the northeast of the island. Between the two hilly regions is a central sedimentary lowland or tableland that is formed by a series of almost horizontally bedded sedimentary rocks of late Miocene/early Pleistocene, the maximum thickness of which is ~100 m (Chen, 1984).

Chinmen kaolin, of sedimentary origin, is an important kaolin deposit with minor residual clays; total reserves are estimated to be >6,000,000 tonnes. The great majority of the kaolin deposits are found in the late Miocene/Pleistocene Chinmen Formation in the central lowland. The kaolin is mined for the pottery industry in Taiwan, and it is the most productive kaolin deposit of the coastal area of the Fukien Province. The aims of this study were to characterize the kaolin deposits and to discuss the genesis of kaolin minerals on the island.

* E-mail address of corresponding author:
mkwang@ccms.ntu.ed u.tw
DOI: 10.1346/CCMN.2004.0520112

GEOLOGICAL SETTING AND OCCURRENCE OF KAOLINS

Geological setting

Chinmen and its neighboring islands are all underlain by granitoid rocks and metamorphosed equivalents. The Mesozoic basement complex of Chinmen Island consists mainly of granitic gneiss (Chen, 1972; Lan *et al.*, 1994, 1995). The geological age ranges from 100 to 139 Ma (Jahn *et al.*, 1976; Lan *et al.*, 1994). The granitic gneiss is composed mainly of quartz, feldspars and micas. The feldspars comprise orthoclase, microcline, acidic plagioclase, and occasionally perthite. Biotite is more abundant than muscovite, and hornblende is only locally important. This basement complex is overlain unconformably by the Chinmen Formation, a succession of Miocene or Pleistocene clastic sedimentary rocks formed by allogenic terrestrial sediments. This formation was deposited in a basin or a paleochannel across the central lowland from coast to coast, and the width of its outcrop belt is ~5 km in an east–west (EW) direction and it covers an area of ~10 km^2. The thickness of this formation, as revealed by drilling, is ~10 m at the eastern border and increases to a maximum of ~100 m in the central area, and then decreases toward the western border. A smaller outcrop of this formation is situated in the White Dragon Creek area on the southeast (SE) coast, adjacent to Liaolo Bay (Figure 1). This outcrop may be a segment of the same channel deposits found in the central lowland, but was isolated by erosion. The Chinmen Formation is, in turn, unconformably overlain by a succession of red-colored sandy muds and gravelly sands that vary from a few m to ~10 m in thickness. This Pleistocene reddish or lateritic sediment that covers the Chinmen Formation forms a tableland. Recent to late

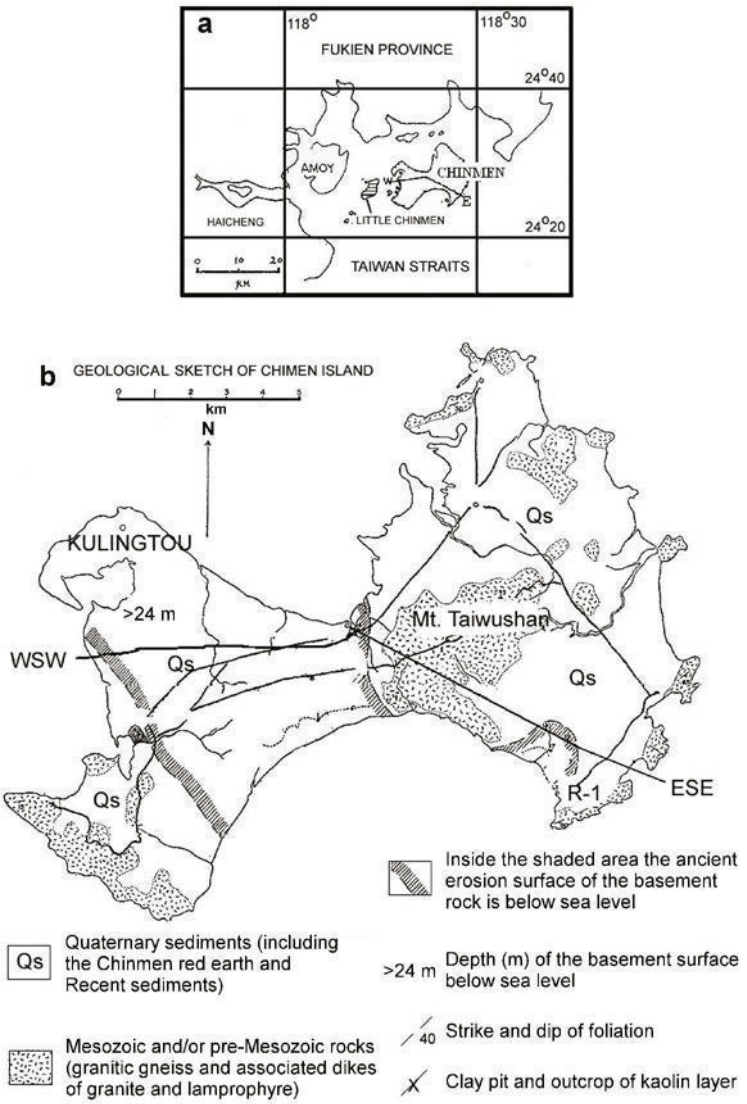

Figure 1. (a) Location map of Chinmen Island, and (b) The WSW–ESE line is the section line of Figure 2 showing the sites of bore holes.

Pleistocene alluvial, coastal and eolian deposits occur locally.

The clastic sediments which make up the Chinmen Formation are chiefly derived from granitic intrusive rocks and rhyolitic flows located along the coast of Fukien Province, China (Ministry of Geology, PRC, 1985). These sediments were deposited on a floodplain near the river mouth and in deltaic channels. Subsequent to the deposition of these sediments, Chinmen Island and the neighboring islets were detached from the coastal area of mainland China by dislocation and erosion.

Occurrence of kaolins

The kaolin clay occurring on Chinmen Island can be divided into two main types, *i.e.* sedimentary (transported) deposits and residual (altered *in situ*) clays.

Sedimentary clays. The Chinmen Formation can be subdivided into two members, namely an upper main member, and a basal member. The basal member is represented by the detrital or lag sediments deposited on the erosional surface of the basement rocks and is composed of abundant degraded mica flakes and quartz sand grains and granules from the basement rocks.

The upper member consists mainly of quartzose sandstone or quartzwacke in the lower part. The interbeds of clay-gall conglomerates are of frequent occurrence in the coarse-grained muddy sandstone. The sandstone is commonly cross-bedded with a kaolinitic, muddy matrix.

The sedimentary sequence becomes finer upward, with the intercalation of fine-grained sandstone, carbonaceous shales and whitish kaolin clays being more

https://doi.org/10.1346/CCMN.2004.0520112 Published online by Cambridge University Press

frequently found. Three layers of whitish kaolin clay have been traced from bore holes, varying from a few cm to ~5 m in thickness, and 3 to 5 km in extent.

Residual clays. There are three types of residual kaolin on Chinmen Island. The first type is kaolin derived from granitic gneiss and the associated igneous dyke rocks, pegmatite, aplite and mafic dykes. This type of kaolinized residual weathering rock is commonly found as a capping of the outcrops of granitic gneiss on the low hills along the ESE coast (Figure 2, R-1). The kaolin contains quartz grains and locally subordinate degraded muscovite. The second type is the red clay formed by lateritic kaolinization developed in a wider area over the island and it may be that this process is still on-going (Figure 2, R-2). The third type is the saprolitic clay altered from the basalt flow in the sea cliff on the islet of Liehyu.

MATERIALS AND METHODS

Materials

Samples of sedimentary clays from the Chinmen Formation were obtained from both the working surface of the clay pits and from core samples (S-1 and S-2 in Figure 2). The residual kaolin samples were collected from outcrops of the kaolinized granitic gneiss, from a few cm to almost 1 m deep (R-1 and R-2 in Figure 2) by chip and channel sampling.

Methods

All samples were disaggregated by shaking in water, and then passed through a #230 sieve (aperture 0.06 mm). The collection of clay-size particles was performed by a gravity settling method according to Stokes' Law (Jackson, 1979). Carbonates, organic matter and free Fe oxides were removed by 0.001 M HCl, 30% H_2O_2 and the citrate-bicarbonate-dithionite (CBD) methods, respectively (Mehra and Jackson, 1960; Kunze and Dixon, 1986). The separated clays were centrifuged, washed three times with 40 mL of deionized water and then freeze dried.

The quantity of illite was estimated from the K_2O content assuming 10% K_2O. Kaolinite was estimated by the XRD peak intensity at 0.72 nm (Brindley, 1980).

X-ray diffraction, differential thermal analysis and electron microscopy

X-ray diffraction (XRD) studies were carried out using a Philips goniometer PW1771 with graphite monochromator. Powder and oriented clay samples were scanned from 4–40º2θ at 2º2θ min^{-1} using CuKα radiation at 35 kV and 15 mA. One hundred samples of the fractionated clays and subordinate raw kaolin clays were analyzed. The Mg-saturated clays were further treated with glycerol solvation to identify expandable clays. The slides of K-saturated clay were heated to 110, 350 and 550ºC for 2 h to characterize the kaolin minerals (Jackson, 1979).

Differential thermal analysis (DTA) was performed using a DuPont 9900 thermal analyzer at a heating rate of 10ºC min^{-1} under air.

Scanning and transmission electron microscopy (SEM and TEM) were used to examine particle morphology. The JSM-35 SEM attached to a Tracor Northern Energy Dispersion Spectrometer (EDS) was employed to view the morphology and perform elemental analysis of kaolins. A single drop of clay suspension was allowed to dry on a copper grid (300 mesh, 3.05 mm diameter) coated with carbon film before examining it with a Hitachi HU12 transmission electron microscope operated at 80 kV.

RESULTS AND DISCUSSION

Kaolin minerals in sedimentary (transported) and residual clays

The basal member of the Chinmen Formation is a micaeous sediment composed of abundant degraded brown biotite flakes, quartz grains and occasional

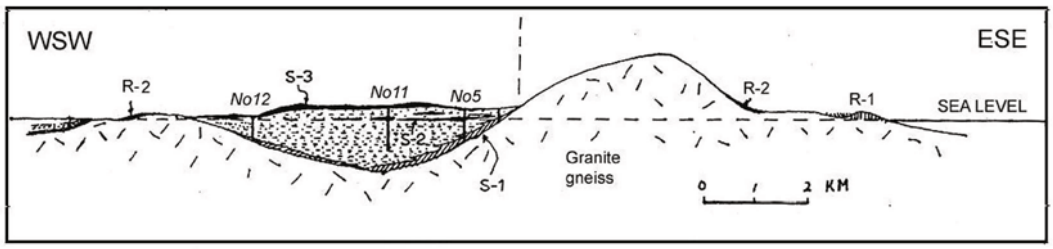

S-1. The basal member of the Chinmen Formation.
S-2. Kaolin beds of the upper Chinmen Formation.
S-3. Latosol and gravel beds of Pleistocene.
R-1. White kaolinized gneissic rock.
R-2. Lateritic kaolins. Nos. 5, 11, 12- Drill number.

Figure 2. A geological cross-section of Chinmen Island showing the distribution of various types of clays and sites of bore holes through the Chinmen Formation along the WSW–ESE line shown in Figure 1b. S-1: Basal deposit on the erosional surface of the basement granitic gneiss; S-2: Sediments with kaolin clays of the Chinmen Formation; S-3; Lateritic kaolin clays overlying the Chinmen Formation. R-1 to R-2: Residual kaolins from outcrops.

https://doi.org/10.1346/CCMN.2004.0520112 Published online by Cambridge University Press

granules of the basement rocks set in a clay matrix (Chen *et al.*, 1972).

The sedimentary kaolins of the Chinmen Formation were characterized as high-defect kaolins. An XRD pattern from a randomly oriented sample is one method for differentiating 0.7 nm halloysite from kaolinite (Brindley, 1980). Compared with the XRD pattern of 0.7 nm halloysite in residual clays (Figure 3), the kaolinite in the Chinmen Formation showed diffuse XRD peaks, without the triplet of diffraction peaks for well crystallized kaolinite at 0.411–0.418 nm and 0.436–0.445 nm. High-defect kaolins show broad peaks in the range 19–23°2θ. The existence of largely high-defect kaolinite on the sedimentary kaolin is diagnosed by the appearance of a diffuse band in the range between 0.412 and 0.445 nm *d* spacings. This diffuse band that slopes to the higher 2θ angle side is composed of four XRD peaks and poorly resolved reflections including 020, $\bar{1}\bar{1}0$, $\bar{1}\bar{1}1$ and $11\bar{1}$ (or 02, 11 of halloysite). Furthermore, two sets of triplet peaks in the range 0.225–0.229 nm are also poorly resolved or even missing. The weak and poorly resolved reflections are generally due to high-defect kaolins (Brindley, 1980) and/or due to fine particle size. This type of XRD pattern characteristic of high-defect kaolinite or halloysite has been documented in the literature (Chen, 1984; Chen *et al.*, 1997; Brindley, 1980; Murray and Keller, 1993). Thus, it was not easy to distinguish between halloysite and kaolinite from the XRD patterns of high-defect kaolins. The XRD results indicated that residual kaolin on the surface of weathered or argillized granitic rock (0–15 cm in depth) is mainly 0.7 nm halloysite

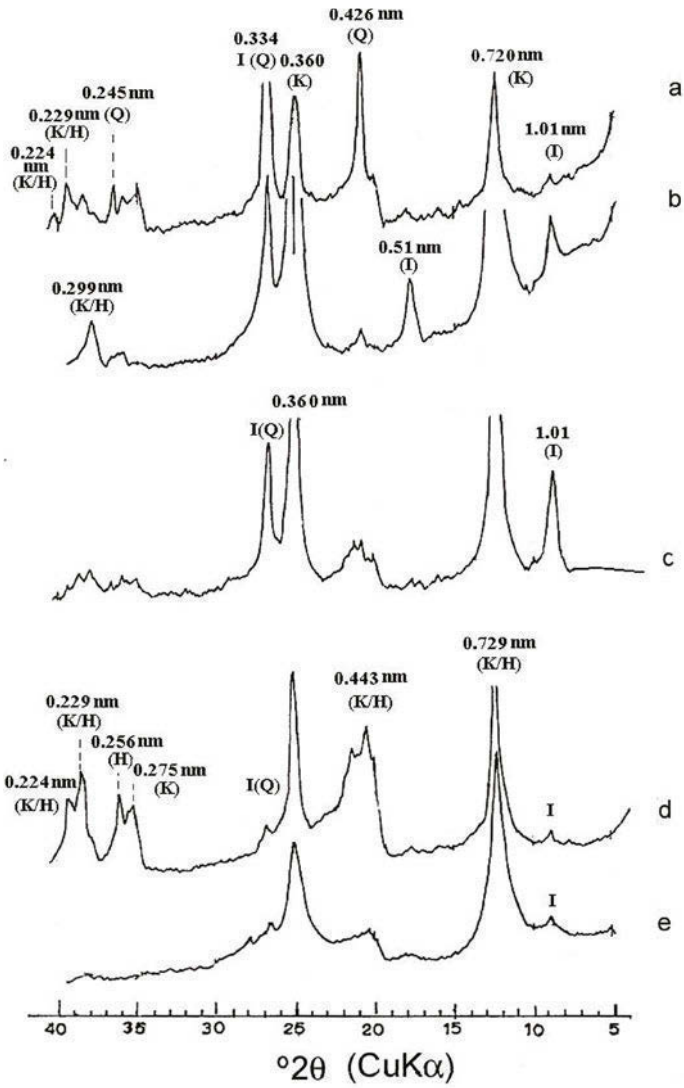

Figure 3. XRD patterns of random powder preparations of kaolin from Chinmen Island: (a) outcrop of the Chinmen Formation and (b) core samples; (c) kaolin from the basal member of the Chinmen Formation; (d) kaolin from argillized granitic gneiss (R-1); (e) kaolin from lateritic argillized granitic gneiss (R-2); H: halloysite; K: kaolinite; Q: quartz; I: illite and S: smectite.

https://doi.org/10.1346/CCMN.2004.0520112 Published online by Cambridge University Press

(Figure 3d,e). In addition, TEM images of halloysite showed the presence of tubular crystals.

Mineral composition of residual clays of gneissoid rocks

The kaolin mineral was probably formed by weathering during early Pleistocene (Chen, 1972). Halloysite, minor kaolinite and illite are the essential components (Figure 3d,e). Better distinction between high-defect kaolinite from 0.7 nm halloysite can be achieved by DTA and electron microscopy.

The DTA curves of the sedimentary clays (S-1 and S-2) (Figure 4a,b) reveal a strong endothermic reaction at 600ºC and a less intensive exothermic peak at ~980ºC. These two reactions may verify the dominant kaolinite content of the samples. There is another very shallow endothermic reaction at ~150ºC (Figure 4a,b), indicating the presence of a minor halloysite mixture in the kaolin (Mackenzie, 1957; Grim, 1968). The DTA curve of a kaolinized pegmatized dike from the locality of R-2 is shown in Figure 4c. In contrast to a and b, the DTA curve in c shows a low-temperature endothermic peak at 150ºC. In addition to the two higher-temperature endothermic and exothermic peaks, this DTA curve verifies that the residual kaolin is composed essentially of halloysite.

Transmission electron microscopy

Clays in the sedimentary deposits are mainly irregular pseudo-hexagonal platelets of kaolinites (Figure 5a,b), while residual clays consist mainly of tubular particles (0.15–0.25 μm in diameter), which are characterized as halloysite (R-2) (Figure 5c,d). Halloysite is relatively less abundant in sedimentary deposits than kaolinite. It is concentrated in the fine size-fraction (Keller, 1977a, 1977b; Bobos *et al.*, 2001), and is lath-like rather than tubular. Some particles are scroll-like in structure, whereas others consist of a bundle of fibers. The diameter (0.1–0.25 μm) of the halloysite tube is similar to that reported by Dixon and McKee (1974), and Dixon (1989). Wang *et al.* (1998), and Singh (1996) proposed a model to explain why halloysite rolls are preferred to tetrahedral rotation for correcting the misfit of the octahedral and tetrahedral sheets. It was shown that the rolling mechanism proceeds when there is significantly less resistance from Si-Si repulsion compared with tetrahedral rotation for correcting the same amount of misfit. Books of loosely stacked assemblages of hexagonal plates in sedimentary kaolinites are often revealed in SEM observations.

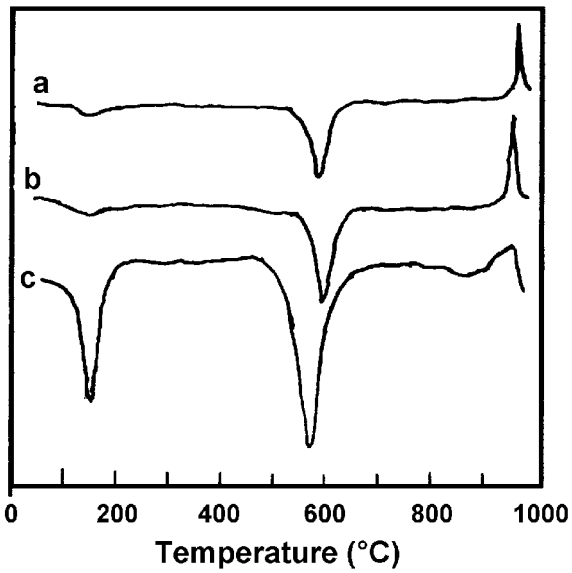

Figure 4. DTA curves of sedimentary clays of (a) S-1, (b) S-2, and (c) kaolinized pegmatized dike of residual clay (R-2).

The results of the randomly oriented XRD analysis, TEM and SEM observations all showed the distinction between the defect kaolinite in sedimentary deposits and 0.7 nm halloysite in residual clays. Singh and Mackinnon (1996) proposed that upon hydration, kaolinite plates roll along the major crystallographic direction to form tubes identical to tubular halloysite. Most tubes are elongated along the *b* crystallographic axis, while some are elongated along the *a* axis. Low-defect particles show a two-layer structure; however, high-defect tubes showed little or no three-dimensional order. Singh (1996) proposed that planar kaolinite transformed to tubular halloysite upon hydration and exfoliation.

Processes of transformation and neoformation

The importance of ion exchange during the transformation is also reflected in the change in chemical composition between terrestrial clays and marine mud. Total chemical analysis of terrestrial and marine mud clays indicates that the SiO_2 content remains constant both before and after transformation (Chen, 1972). The loss of Al from the marine mud is probably due to the dissolution of Al_2O_3 after the decomposition of high-defect kaolins and amorphous materials. Magnesium and K^+ are somewhat increased due to the increased amount of illite and chlorite-vermiculite-montmorillonite minerals. The Mg^{2+}/K^+ ratio of marine mud is much higher than that of terrestrial clays. The diagenetic change of marine clay with depth was noted in some core samples. The decrease in the 0.7 nm/1.0 nm ratio with depth indicates increasing quantity and/or enhanced crystallinity of illite and its interstratified phase by recrystallization after long burial (Chen, 1972).

Kaolinization of granitoid rocks

Muscovite flakes and alteration products were observed by SEM (Figure 6). With the exception of some dispersed particles, most halloysite tubes are associated with mica flakes. These elongated crystals grow as upright filaments in the basal cleavage planes or

https://doi.org/10.1346/CCMN.2004.0520112 Published online by Cambridge University Press

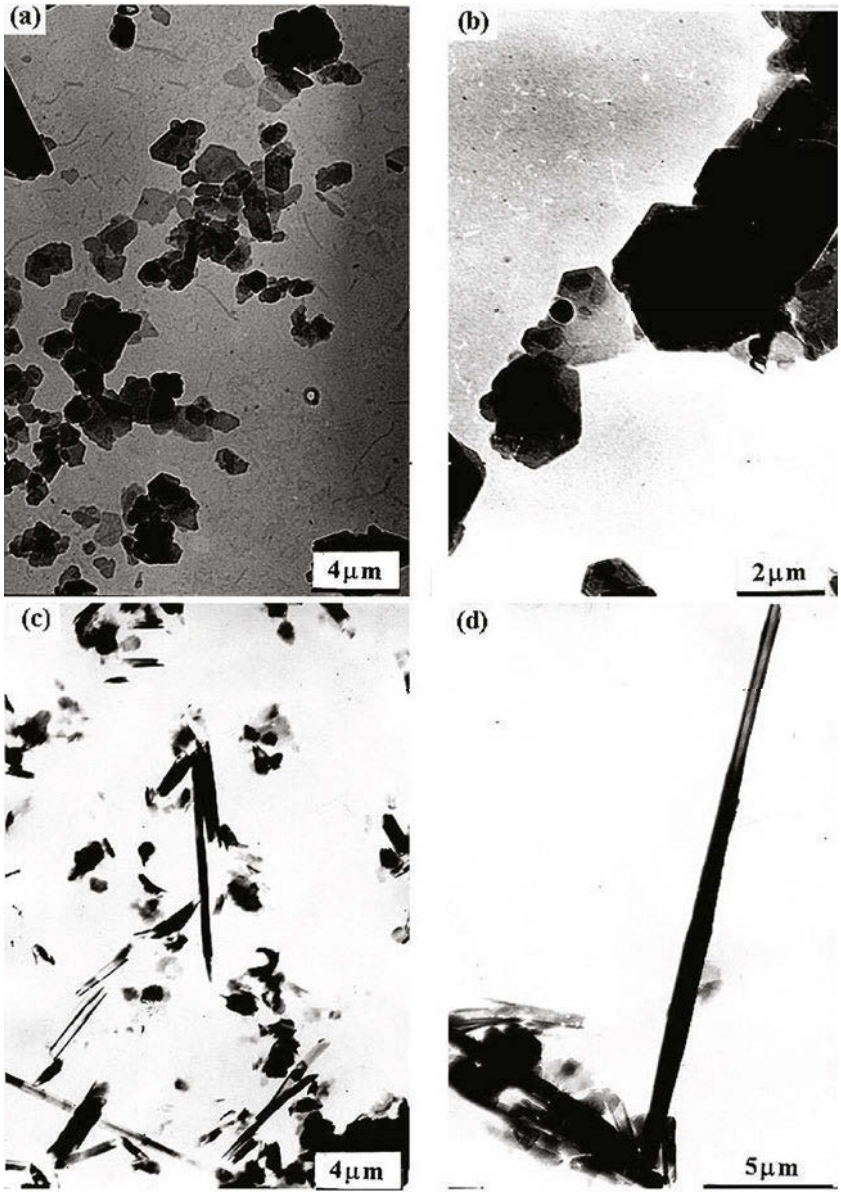

Figure 5. TEM images of (a) kaolin platelets from the kaolin beds of Chinmen Formation; (b) core samples; (c) halloysite from R-1, and (d) halloysite from R-2.

on the edges of the mica flakes (Figure 6b,c). It was also found that some elongated particles were apparently formed by another process. Some mica flakes were found being split into parallel slender laths. Moreover, all individual flakes of a cluster are split along a common trend or orientation. It is possible that splitting was induced by mechanical shattering of the kaolinized rock under stress.

Observation of kaolins in sedimentary and residual clays are summarized as follows:

(1) Aggregates of kaolinite are characterized by their common occurrence and distinctive fan-shaped composite stacks or coalesced stacks which are closely associated with mica plates. This mode of occurrence implies that the parallel growth of kaolinite stacks originated on the edges of the mica plates and were pseudomorphous after mica by topotactic growth (Glasser *et al.*, 1963; Bernal and Mackay, 1965). Later, the coalesced stacks on the fringes of the altered mica plates split apart successively into discrete stacks.

(2) Most of the particles with a micaceous platy morphology are likely to be identified as halloysite. As revealed by chemical analysis, it always contains a small amount of K inherited from the mica (Chen *et al.*, 1997).

(3) The residual granite showed pitted surfaces or a spongy structure. However, these grains are rather clean and devoid of any kaolinite-like particles on their surface. This indicates that they have been corroded by

https://doi.org/10.1346/CCMN.2004.0520112 Published online by Cambridge University Press

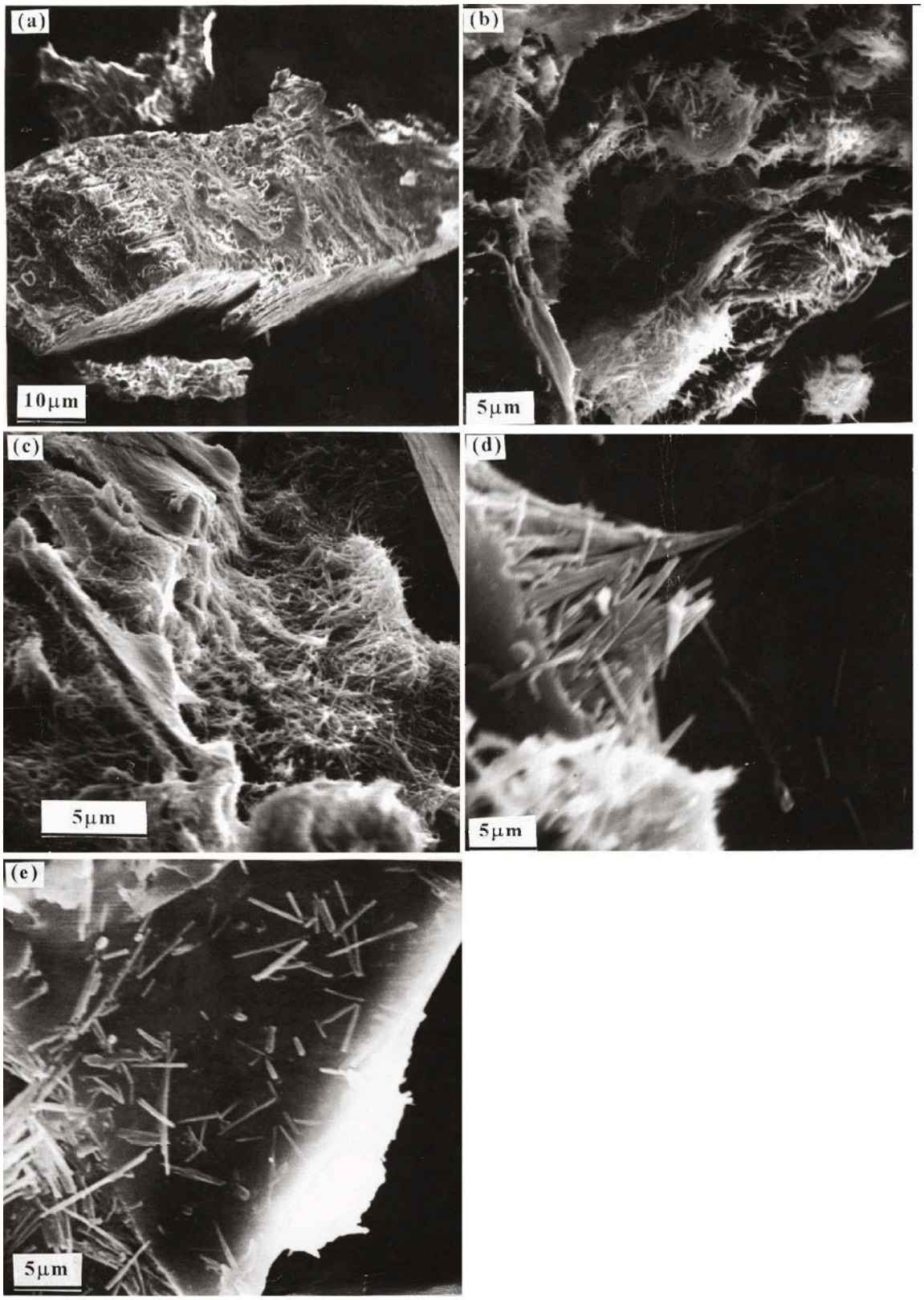

Figure 6. SEM images of (a) muscovite mica flakes, (b) alteration of mica to kaolinite, (c) and (d) the elongated halloysite associated with mica, and (e) halloysite distributed on the cleavage surface of mica.

https://doi.org/10.1346/CCMN.2004.0520112 Published online by Cambridge University Press

acidic solutions, and are thus not directly related to kaolin mineral formation.

Kaolinitization of granite by weathering is widely accepted as the most important source of kaolin (Grim, 1968; Riedmuler, 1978). Weathering of the mica and residual feldspars result in the transformation to kaolin. Most of the mica flakes are only partly split along cleavage traces and/or have frayed edges. Thick micaceous books subject to alteration were first exfoliated into thinner books or individual sheets. The thin sheets later tended to become frayed at their edges or fan out on one side as a result of hydration, K depletion and expansion.

CONCLUSIONS

The main kaolin bed is the upper member of the Chinmen Formation. The kaolin bed is associated with weakly consolidated, immature, quartzose sandstone, and is distributed essentially within a broad Pleistocene valley which runs through the central part of Chinmen Island. The clay mineral composition of the kaolin bed consists mainly of high-defect kaolinite associated with illite. These clays are detrital in origin and were derived from a low-relief, mainly granitic (granite, pegmatite and rhyolite) source area, and the sediments represent floodplain deposits near a river mouth. The genesis of kaolins in Chinmen Island is valuable and merits further study.

ACKNOWLEDGMENTS

This study was supported by the National Science Council, Taiwan, Republic of China, under projects NSC 89-2621-B-002-006 and 89-2621-B002-019. We are indebted to Professor P.M. Huang (Emeritus Professor of Soil Science, University of Saskatchewan, Canada) for his insightful comments and critical reading of the manuscript.

REFERENCES

Bernal, J.D. and Mackay, A.L. (1965) Topotaxy. *Tschermaks Mineralogie und Petrographic Mitteuropean*, **10**, 331–340.

Bobos, I., Duplay, J., Rocha, J. and Gomes, C. (2001) Kaolinite to halloysite-7 Å transformation in the kaolin deposit of São Vicente de Pereira, Portugal. *Clays and Clay Minerals*, **49**, 596–607.

Brindley, G.W. (1980) Order-disorder in clay mineral structures: Pp. 125–195 in: *Crystal Structures of Clay Minerals and their X-ray Identification* (G.W. Brindley and G. Brown, editors). Monograph **5**. Mineralogical Society, London.

Chen, P.Y. (1972) Clay minerals from the alterations of mafic and intermediate igneous rocks in Taiwan and neighboring islands. *Proceedings of the Geological Society of China*, **15**, 45–64.

Chen, P.Y. (1984) Distribution and origin of clay minerals in the shallow sea surrounding the Chinmen Island (Quemoy), Fukien, China. *Proceedings of the Geological Society of China*, **27**, 101–118.

Chen, P.Y., Lin, M.-L. and Zheng, Z. (1997) On the origin of the name kaolin and the kaolin deposits of the Kauling and Dazhou areas, Kiangsi, China. *Applied Clay Science*, **12**, 1–25.

Dixon, J.B. (1989) Kaolin and serpentine group minerals. Pp. 127–137 in: *Minerals in Soil Environments* (J.B. Dixon and S.B. Weed, editors). Soil Science Society of America, Madison, Wisconsin.

Dixon, J.B. and McKee, T.R. (1974) Internal and external morphology of tubular and spheroidal halloysite particles. *Clays and Clay Minerals*, **22**, 127–137.

Glasser, L.S.D., Glasser, F.P. and Taylor, H.F.W. (1963) *The Role of Oriented Transformations in Mineralogy*. Special Paper **1**. Mineralogical Society of America, Washington, D.C. pp. 200–263.

Grim, R.E. (1968) *Clay Mineralogy*. McGraw-Hill, New York, 596 pp.

Jackson, M.L. (1979) *Soil Chemical Analysis – Advanced Course*. 2nd edition. University of Winconsin, Madison, Wisconsin, 497 pp.

Jahn, B.M., Chen, P.Y. and Yen, T.P. (1976) Rb-Sr ages of granitic rocks in South eastern China and their tectonic significance. *Geological Society of America Bulletin*, **86**, 763–776.

Keller, W.D. (1977a) Scan electron micrographs of kaolins collected from diverse environments of origin. Part 3. *Clays and Clay Minerals*, **25**, 262–264.

Keller, W.D. (1977b) Scan electron micrographs of kaolins collected from diverse environments of origin. Part 4. *Clays and Clay Minerals*, **25**, 311–345.

Kunze, G.W. and Dixon, J.B. (1986) Pretreatment mineralogical analysis. Pp. 91–100 in: *Methods of Soil Analysis. Part 1* (2nd edition) (A. Klute, editor). Agronomy Monographs Series, **9**. American Agronomy Society, Madison, Wisconsin.

Lan, C.-Y., Chung, S.-L., Mertzman, S.A. and Hsu, W.-Y. (1994) Petrology, geochemistry and Nd-Sr isotope of late Miocene basalts in Liehyu and Chinmen, Fukien. *Journal of the Geological Society of China*, **37**, 309–334.

Lan, C.-Y., Chung, S.-L., Mertzman, S.A. and Chen, C.-H. (1995) Mafic dikes from Chinmen and Liehyu islands off southeast China: Petrochemical characteristics and tectonic implications. *Journal of the Geological Society of China*, **38**, 183–213.

Mackenzie, R.C. (1957) *The Differential Thermal Investigation of Clays*. Monograph **2**. Mineralogical Society, London, 456 pp.

Mehra, O.P. and Jackson, M.L. (1960) Iron oxides removed from soils and clays by a dithionite-citrate system buffered with sodium bicarbonate. *Clays and Clay Minerals*, **7**, 317–327.

Ministry of Geology, P.R.C. (1985) Regional Geology of Fukien Province. *Geological Memoirs*, Series 1, no. 4, Geology. Publishing House, Beijing, China.

Murray, H.H. and Keller, W.D. (1993) Kaolins, kaolins and kaolins. Pp. 1–24 in: *Kaolin Genesis and Utilization* (H.H. Murray *et al*., editors). Special Publication **1**. Clay Minerals Society, Boulder, Colorado.

Riedmuler, G. (1978) Neoformations and transformations of clay minerals in tectonic shear zones. *Tschermaks Mineralogie und Petrographic Mitteuropean*, **25**, 219–242.

Singh, B. (1996) Why does halloysite roll? A new model. *Clays and Clay Minerals*, **44**, 191–196.

Singh, B. and Mackinnon, I.D.R. (1996) Experimental transformation of kaolinite to halloysite. *Clays and Clay Minerals*, **44**, 825–834.

Wang, W.M., Yeh, H.W., Chen, P.Y. and Wang, M.K. (1998) Kaolin mineralogy of clays in paleosol profile on the Late-Miocene sediments in Penghu islands (Pescadores), Taiwan. *Clays and Clay Minerals*, **46**, 1–9.

(*Received 1 November 2002; revised 22 July 2003; Ms. 733*)